



Optimization of Freewheeling Device Implementation in SiC MOSFETs

Design Summary

Objectives

This paper discusses the optimization of freewheeling device implementation for SiC MOSFETs in a half-bridge configuration. It presents the dynamic characterization of multiple freewheeling device implementations with SiC MOSFET switching. The behaviors of SiC MOSFET body diode and SiC Schottky barrier diode (SBD) are compared with switching devices of SiC MOSFETs with and without Kelvin source connections. This paper aims to determine whether the body diode of a SiC MOSFET is a limiting factor for high speed switching of MOSFETs.

Applications

- General-purpose inverters
- Motor drives
- PV inverters
- UPS
- DC-DC converters
- Switching mode power supply

Target Audience

This document is intended for potential adopters of SiC MOSFETs to help them determine the ideal freewheeling device implementation that optimizes system efficiency and power semiconductor cost.

Contact Information

For more information on the topic of optimizing the implementation of Freewheeling Devices in SiC MOSFET applications, contact the Littelfuse Power Semiconductor team of product and applications experts:

- PowerSemiSupport@Littelfuse.com

Table of Contents

| | |
|--|----|
| 1. Introduction | 3 |
| 2. Characterization Circuits | 4 |
| 3. Comparing Pulse Testing Performance of Switching Devices | 6 |
| 4. Comparing Pulse Testing Performance of Freewheeling Devices | 8 |
| 5. Continuous Operation Test Comparison | 9 |
| 6. Freewheeling Device Selection | 10 |
| 7. Conclusion | 11 |
| 8. References | 11 |

List of Figures

| | |
|---|----|
| Figure 1. Device Structure of SBD and MOSFET | 3 |
| Figure 2. Freewheeling Device Implementation Configurations | 4 |
| Figure 3. Pulse Testing Platform | 5 |
| Figure 4. Continuous Test Platform | 6 |
| Figure 5. Switching Waveform Comparison Between Different Freewheeling Device Implementations | 7 |
| Figure 6. Switching Loss Comparison between Different Freewheeling Device Implementations | 8 |
| Figure 7. Waveforms of Freewheeling Devices at 20 A Load Current under 25 °C and 150 °C | 9 |
| Figure 8. Converter Loss Comparison of 3L and 4L MOSFETs Switching with and without SBD as Antiparallel Diode | 10 |
| Figure 9. I-V Characteristics Comparison of SiC MOSFET Body Diode and SiC SBD | 11 |

1. Introduction

Silicon Carbide (SiC) power devices outperform Si devices in several aspects, with features such as lower switching loss and low temperature dependence. The wide bandgap feature of SiC material enables unipolar device implementation for higher voltage applications (>600 V), which eliminates minority carrier extraction during forced device turn-off. SiC MOSFETs and Schottky Barrier Diodes (SBD), shown in Figure 1, offer promising potential for high-efficiency high power density converter designs due to their superior performance over Si devices.

For SiC SBD, as shown in Figure 1 (a), the Reverse Recovery (RR) behavior due to minority carrier extraction during forced diode turn-off can be eliminated, as compared with the Si P-N junction diode. The quasi “reverse recovery” charge is only related to the device output capacitance. The switching losses are ultra-low, and they are independent of di/dt , current level, and temperature. However, the on-state voltage drops on SiC SBD are relatively high due to the wide-bandgap feature of SiC material, which results in a relatively high conduction loss on SBD. The use of half-bridge configuration and synchronous rectification can reduce conduction loss effectively and improve system efficiency and is therefore widely adopted in high performance systems.

SiC MOSFET devices have no tail current during device turn-off, resulting in a much lower turn-off loss compared with IGBT. Moreover, SiC MOSFETs have an intrinsic body diode, so it is not necessary to add an antiparallel diode. The body diode of a SiC MOSFET is still a P-N structure [4] with a reverse recovery charge that is dependent on di/dt , current level, and temperature. However, the minority carrier lifetime in SiC is much shorter than in Si. Consequently, the reverse recovery behavior in SiC devices is less significant than in Si devices at low temperature and normal switching speed. Therefore, the reverse recovery behavior of the SiC SFET body diode can still be observed under high temperature and high current density working conditions.

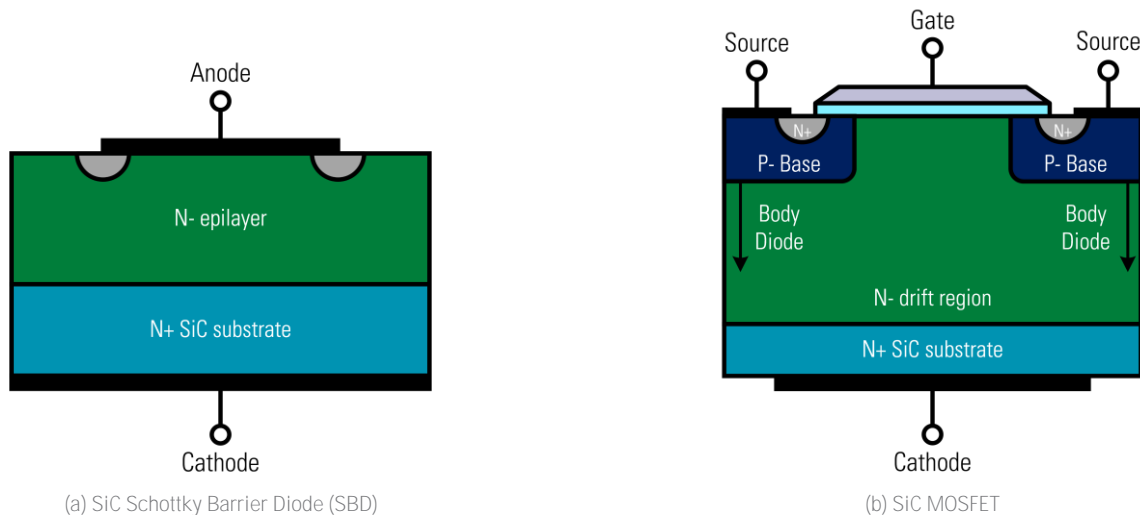


Figure 1. Device Structure of SBD and MOSFET

For SiC MOSFETs, it is desirable to have a higher switching speed to reduce switching loss and a higher junction temperature to reduce the cooling system. Therefore, utilizing a body diode may limit the advantages of system loss reduction provided by SiC MOSFETs. Adding an antiparallel SBD to SiC MOSFET, as shown in Figure 2 (c), may be necessary, but could increase the total capacitive charge and increase switching loss under low temperature. It would also increase the total cost of the system. Recently, new discrete packages with dedicated gate source pins called Kelvin Source (KS) connections, as shown in Figure 2 (e), have been developed to further increase the switching speed of SiC MOSFETs and reduce the gate loop noise coupling. These new packages include the four-lead (4L) TO-247 packages, seven-lead (7L) TO-263 packages and Surface Mount Power Device (SMPD) packages. In addition, almost all the module packages have a dedicated gate source pin for SiC MOSFETs. With a Kelvin source connection, the switching speed of SiC MOSFETs can be three to eight times faster than that of traditional 3L packages. Because the body diode reverse recovery behavior is highly dependent on the speed of minority carrier extraction, faster device turn-on speed will induce more serious reverse recovery during freewheeling diode turn-off. The behavior of the body diode of SiC MOSFETs with Kelvin source connections will be different to that of traditional packages without Kelvin source connections.

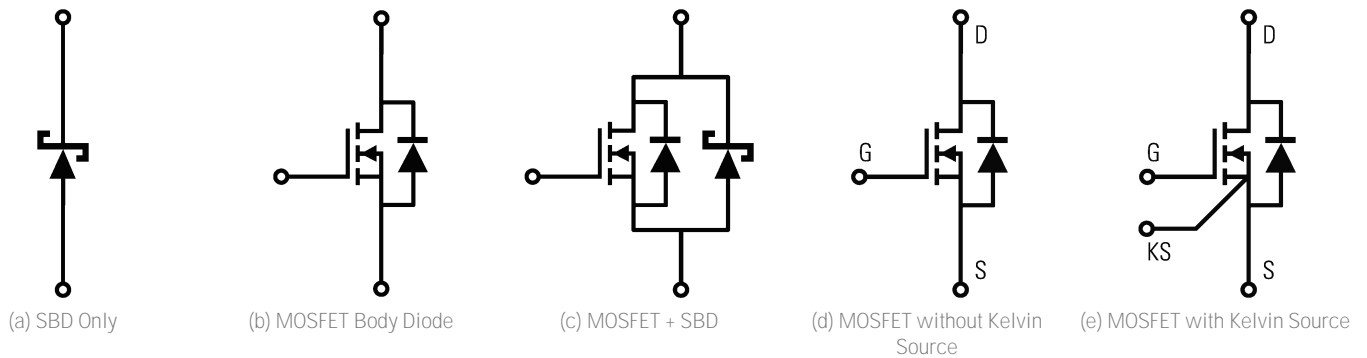
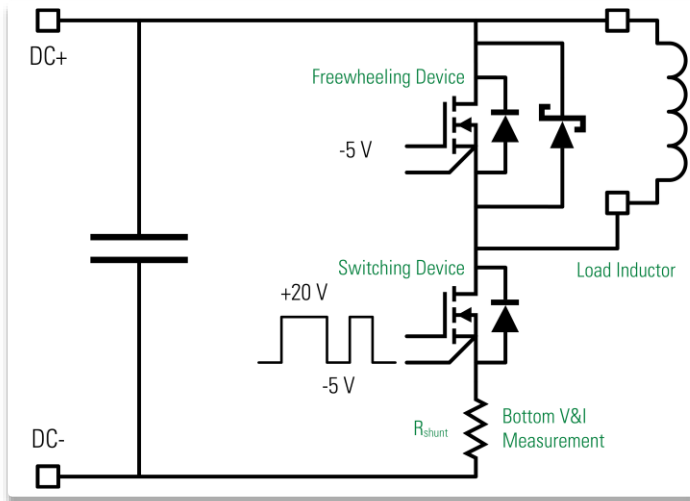


Figure 2. Freewheeling Device Implementation Configurations

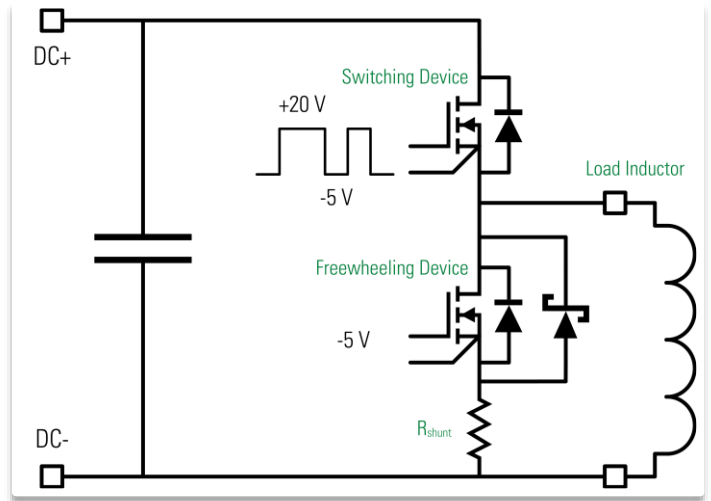
This document aims to test whether the body diode of a SiC MOSFET is a limiting factor for high speed switching of MOSFETs with Kelvin source connections. It presents the dynamic characterization of the SiC MOSFET body diode and Schottky diode with loss and charge comparison of various freewheeling device implementations under different temperatures. Two characterization platforms were developed to measure the pulse switching energy and continuous switching efficiency of a ‘phase leg’ SiC MOSFET’s stage with different freewheeling device implementations, including the SiC MOSFET body diode with and without anti-parallel Schottky Barrier Diodes (SBD). The switching energy and converter efficiency results are presented to quantify the benefits of adding antiparallel SBD in loss reduction and EMI noise mitigation for SiC MOSFETs with Kelvin source connections under different switching conditions. Based on the comparison results, a design guideline is provided to assist in the selection of a freewheeling diode with minimal switching losses of SiC devices. The experimental tests were performed on a 4L-TO-247 package to increase the switching speed of SiC MOSFETs. Results would also apply to other discrete packages with Kelvin connection and SiC MOSFETs in power module designs operated at similar switching speeds.

2. Characterization Circuits

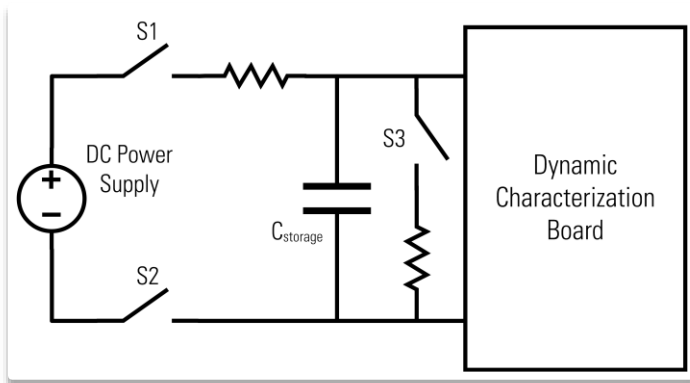
To measure and compare the performance of different freewheeling device implementations, two test platforms were developed to evaluate the pulse switching performance and continuous operation performance separately. Figure 3 shows the schematics of the pulse testing platform. The pulse test platform uses a half-bridge configuration with separate gate drivers for top and bottom devices. Each switching position can be either MOSFET or SBD and MOSFET in parallel. The MOSFET socket can hold both 3L and 4L TO-247 devices for a fair comparison with the same power loop design. The test platform can be configured in different ways to measure switching loss and freewheeling charge separately. Figure 3 (a) and Figure 3 (b) represent the different configurations for measuring switching loss and reverse recovery charge separately. The pulse test platform can measure either switching device behavior or freewheeling device behavior by changing the configurations. For the switching device measurement (Figure 3 (a)), the bottom device is driven with a double pulse gate signal and the top device is freewheeling. For the freewheeling current measurement (Figure 3 (b)), the top device switches with the double pulse gate signal and the bottom device is freewheeling. Therefore, both switching loss and freewheeling charge can be calculated based on the measured voltage and current waveform. To ensure the accuracy of current and voltage measurement during the switching transient, a low inductance and high bandwidth shunt resistor is connected in series with the bottom device to measure the current transient during switching or freewheeling. A passive high bandwidth voltage probe is plugged into a probe tip adapter that is soldered near the bottom device for accurate voltage measurement during the switching transient. The voltage probe and current shunt is connected to one common measurement ground which is different from the power circuit negative bus. To avoid high frequency, the circuit current propagates between measurement ground and power ground. The power circuit in the measurement setup is floated using a capacitor bank, as shown in Figure 3 (c). Switch S1 and S2 is ON to charge the DC link voltage to the desired value. During testing, switch S1 and S2 is OFF to ensure the power loop is float and the whole system is single grounded by the oscilloscope through the measurement ground of voltage probe and shunt resistor S3 to control the discharge of the DC link capacitor when the test is completed. Figure 3 (d) shows the actual hardware of the pulse test platform.



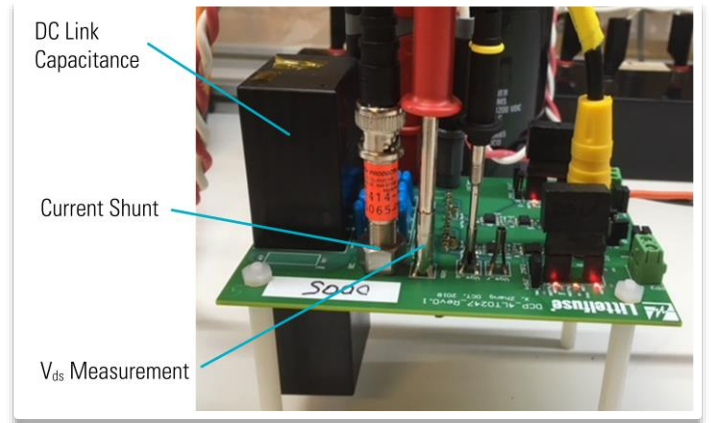
(a) Configuration for Switching Loss Measurement



(b) Configuration for Charge Measurement



(c) Circulating Current Reduction

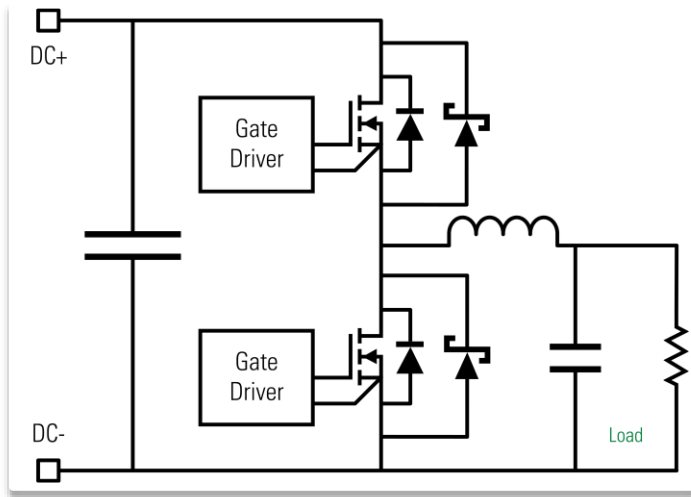


(d) Hardware Setup

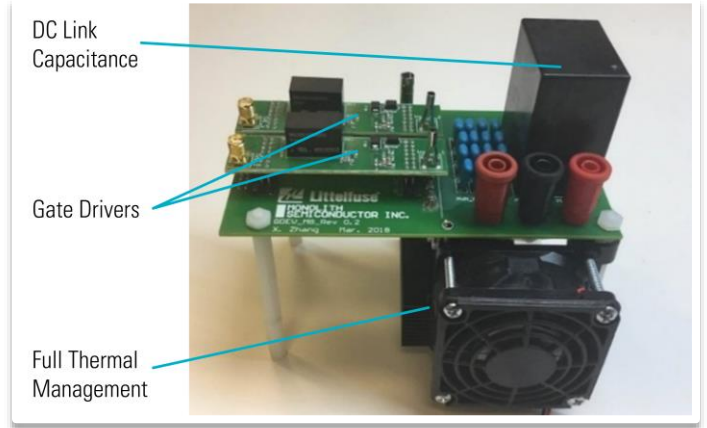
Figure 3. Pulse Testing Platform

Figure 4 shows the schematics and the actual hardware of the continuous test platform. The continuous test platform also features a half-bridge configuration with separate gate drivers for the top and bottom switches. It has a full thermal solution that enables high power delivery with continuous high frequency switching. In the measurement, the platform runs in a buck configuration with synchronous rectification and the platform is connected with an RLC load. The input and output DC voltage and current are measured using a power analyzer for converter efficiency measurement. The power loss includes the power loss of the power semiconductors and the loss on the passive components. With different freewheeling device implementations, the passive component loss is the same under the same operational conditions. Therefore, the difference in the total power loss will indicate the loss difference of various freewheeling device implementations.

In both setups, each SiC MOSFET is driven by a gate driver IC with a signal isolator IC for proper driving performance and good noise isolation. Both gate loop and power loop are minimized by reducing the loop length and overlapping the current return path to avoid excessive voltage overshoot due to loop inductance.



(a) Circuit Configuration



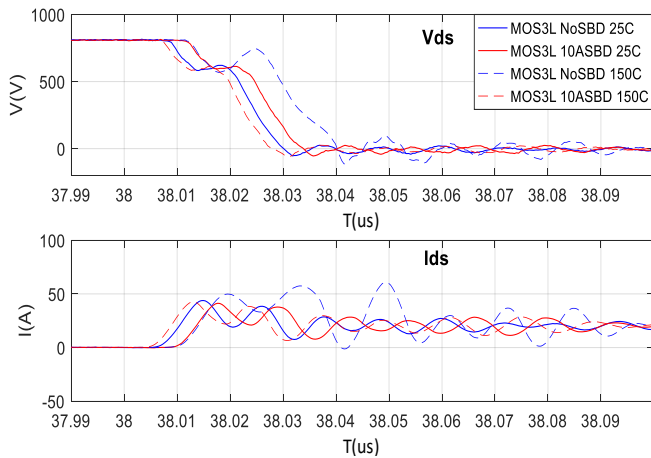
(b) Hardware Setup

Figure 4. Continuous Test Platform

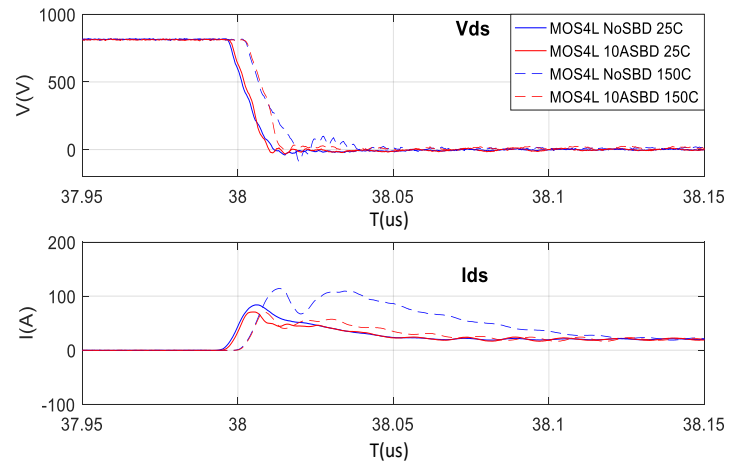
3. Comparing Pulse Testing Performance of Switching Devices

The pulse test platform is used to measure the dynamic performance of the switching devices (1200 V SiC MOSFET LSIC1MO120E0080). Test conditions are $V_{dc}=800\text{ V}$, driving voltage $V_{gs} = +20\text{ V}/-5\text{ V}$, external gate resistance $R_g = 1\text{ Ohm}$, testing temperature $25\text{ }^\circ\text{C}/150\text{ }^\circ\text{C}$, load current $10\text{ A}-40\text{ A}$. For loss measurement, the low side device is switched and measured, while the high side device is freewheeling, as shown in Figure 3 (a). The switching loss of the bottom MOSFET is compared between two different top freewheeling device implementations -- using only the body diode of MOSFET and using the body diode of MOSFET in parallel with 10 A SiC SBD.

Figure 5 shows the 3L and 4L MOSFET turn-on current and voltage with different freewheeling device configurations at different temperatures. For the 3L MOSFET switching condition, adding SBD at $25\text{ }^\circ\text{C}$ provides no benefit in reducing the current overshoot as temperature and switching speed are low. Adding SBD at $150\text{ }^\circ\text{C}$ can reduce the current overshoot due to reverse recovery; however, the benefit is limited due to the lower switching speed. 4L MOSFET switching with body diode shows high peak current during switching when the load current is 20 A . The peak current reaches 80 A at $25\text{ }^\circ\text{C}$ and greater than 100 A at $150\text{ }^\circ\text{C}$. This indicates that there is a significant reverse recovery charge when freewheeling using only the body diode of SiC MOSFET. Compared with the 3L package switching results, the 4L package shows five times faster di/dt than the 3L package under the same driving parameters and the same switching current, which induces a much higher reverse recovery current in the body diode. Adding a 10 A antiparallel SBD eliminates the RR charge, making the peak current less than 50 A at $150\text{ }^\circ\text{C}$. Even at $25\text{ }^\circ\text{C}$, adding SBD effectively reduces the current overshoot and switching loss energy.



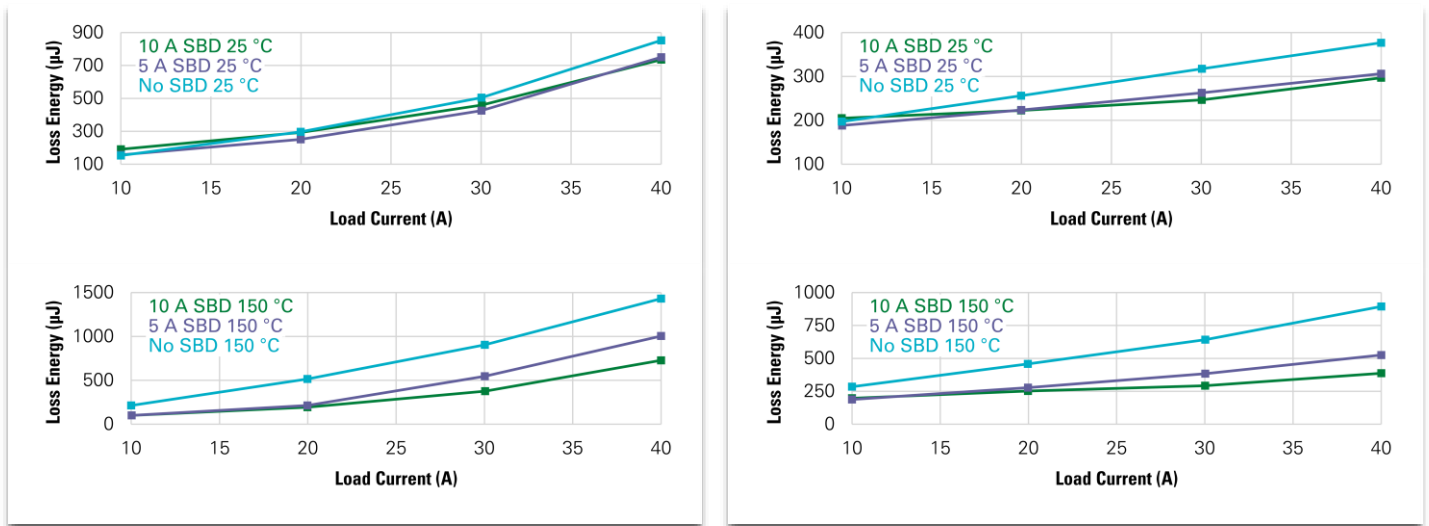
(a) Turn-on Waveforms of 3L MOSFET at 20 A under 25 °C and 150 °C



(b) Turn-on Waveforms of 4L MOSFET at 20 A under 25 °C and 150 °C

Figure 5. Switching Waveform Comparison Between Different Freewheeling Device Implementations

Figure 6 shows a comparison of the switching loss between different freewheeling device implementations with 3L and 4L MOSFET switching at different operating temperatures. For 3L MOSFET switching at 25°C, adding only SBD has a limited benefit on loss reduction at higher load (>30 A). At a 10 A load condition, adding a 5 A SBD only helps reduce switching loss by 5%; however, adding a 10 A SBD increases switching loss by 2.5%. This is mainly because, by adding the SBD capacitance to the switching device output capacitance, the total output capacitance of the freewheeling device increases switching loss, which counters the reduction of reverse recovery induced switching loss. For low load current switching conditions, the reverse recovery induced loss is not dominant. The increase in switching losses from adding a 10 A SBD is greater than the reduction of reverse recovery induced switching loss. Therefore, adding a 10 A SBD makes the total loss even higher. The selection of proper SBD rating is discussed in Section 6. Freewheeling Device Selection.



(a) Turn-on Loss Comparison of 3L MOSFET at 25 °C and 150 °C

(b) Turn-on Loss Comparison of 4L MOSFET at 25 °C and 150 °C

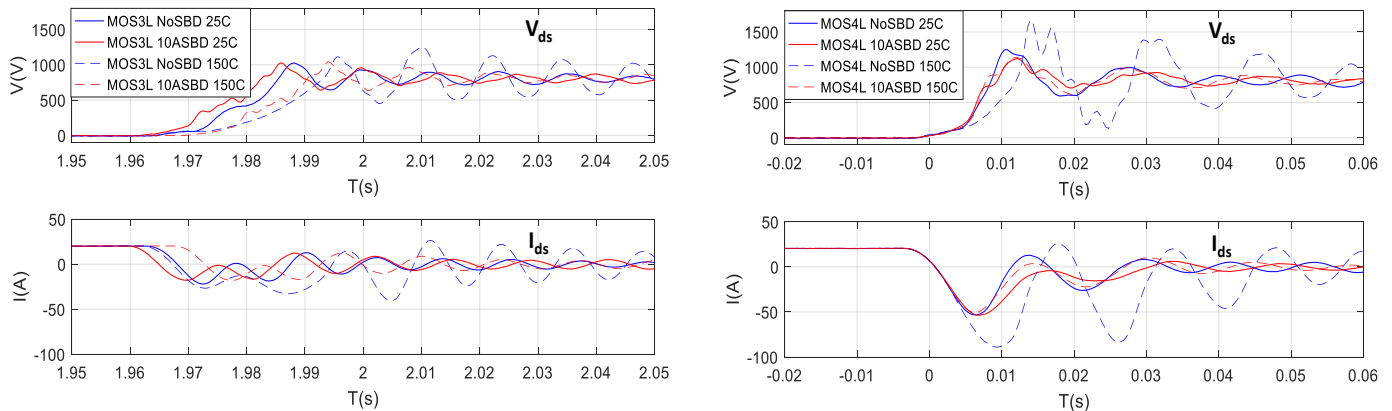
Figure 6. Switching Loss Comparison between Different Freewheeling Device Implementations

4. Comparing Pulse Testing Performance of Freewheeling Devices

The pulse test platform can also measure the dynamic performance of the freewheeling devices. For freewheeling device measurement, the arrangement of Figure 3 (b) is used with the top device switched and the bottom device freewheeling. By measuring the freewheeling device voltage and current, the Reverse Recovery (RR) behavior such as RR charge, RR peak current, and RR time can be characterized.

Figure 7 shows the measured freewheeling waveforms with 3L and 4L MOSFET switching at different temperatures. The current waveform below zero is due to forced turn-off of the freewheeling device – this current is the sum of both output capacitance discharge current and P-N junction reverse recovery current. For 3L MOSFET switching conditions, under room temperature, adding a 10 A SBD has no significant impact on voltage overshoot and current undershoot. This indicates that the reduction of reverse recovery charge is comparable to the increase of total output capacitance charge. For an operating temperature of 150 °C, adding a 10 A SBD can reduce the voltage overshoot and current overshoot slightly since the reverse recovery charge increases at higher temperature. For 4L MOSFET switching conditions, when only the body diode is used as the freewheeling device, 4L device switching has a much higher current undershoot due to the faster switching speed compared with 3L device switching. Meanwhile, the voltage overshoot is also much higher for the 4L switching condition due to the higher di/dt value.

These results confirm that the reverse recovery charge is more dominant for 4L device switching. At 150 °C temperature, the peak reverse recovery current undershoot is more than -90 A and the voltage overshoot is higher than 1500 V due to higher di/dt. The high current and high voltage ringing at high frequency will increase converter EMI noise emission. With a 10 A SBD antiparallel diode, there is less difference between 25 °C and 150 °C operations. because adding an SBD eliminates the reverse recovery charge of the body diode during forced turn-off. The total capacitive discharge current is independent of temperature and load current. Results also show that adding an antiparallel SBD can reduce both voltage and current ringing significantly during switching transients. This may help to reduce the EMI noise emission radiating from phase leg connections.



(a) 3L MOSFET Switching with Different Freewheeling Device Implementation (b) 4L MOSFET Switching with Different Freewheeling Device Implementation

Figure 7. Waveforms of Freewheeling Devices at 20 A Load Current under 25 °C and 150 °C

5. Continuous Operation Test Comparison

The performance of multiple freewheeling device implementations for different packages is compared in real converter applications using the continuous test platform discussed in Section 2. Characterization Circuits. The system is configured as a hard-switched buck converter with synchronous rectification and fixed 50% duty cycle fixed frequency PWM control. The load is swept by varying the load resistor value. A power analyzer is used to measure the input and output power to calculate the total loss. The total loss includes semiconductor switching and conduction loss and all passive component loss. Even when the freewheeling device implementation is realized differently, the passive component loss remains the same. The total loss difference indicates the semiconductor loss difference. Test conditions are: $V_{in} = 800\text{ V}$, $V_{out} = 400\text{ V}$, $V_{gs} = +20\text{ V}/-5\text{ V}$, $R_g = 1\text{ Ohm}$, $f_s = 100\text{ kHz}$, Load $L = 710\text{ }\mu\text{H}$, output power = 400 W–5 kW. Figure 8 shows the loss comparison of 3L and 4L MOSFETs with and without SBD as antiparallel diode. For 3L MOSFET switching, adding a 5 A diode increases the converter loss over the whole load range. Even at 5 kW output power, the device average current is about 6.25 A. Previously, in Section 3. Comparing Pulse Testing Performance of Switching Devices, it was shown that the reverse recovery loss reduction is lower than the loss increments due to the added output capacitance under this low current. Therefore, there is no benefit derived from adding an antiparallel diode to 3L devices for these conditions. However, 4L MOSFETs' switching converters have different results. The reverse recovery loss is more dominant due to a much faster switching speed. The results indicate that adding a 5 A SBD diode will increase loss at light load (<3.2 W). The loss will become lower when the load increases (>3.2 kW). This is because at higher load current and higher device temperature, the reverse recovery induced loss increases. When load current and device temperature increases, the benefit of adding an SBD also increases. The continuous test results complement the pulse test results. The current rating of the antiparallel SBD needs to be optimized, as adding a larger SBD will increase the switching loss at light load.

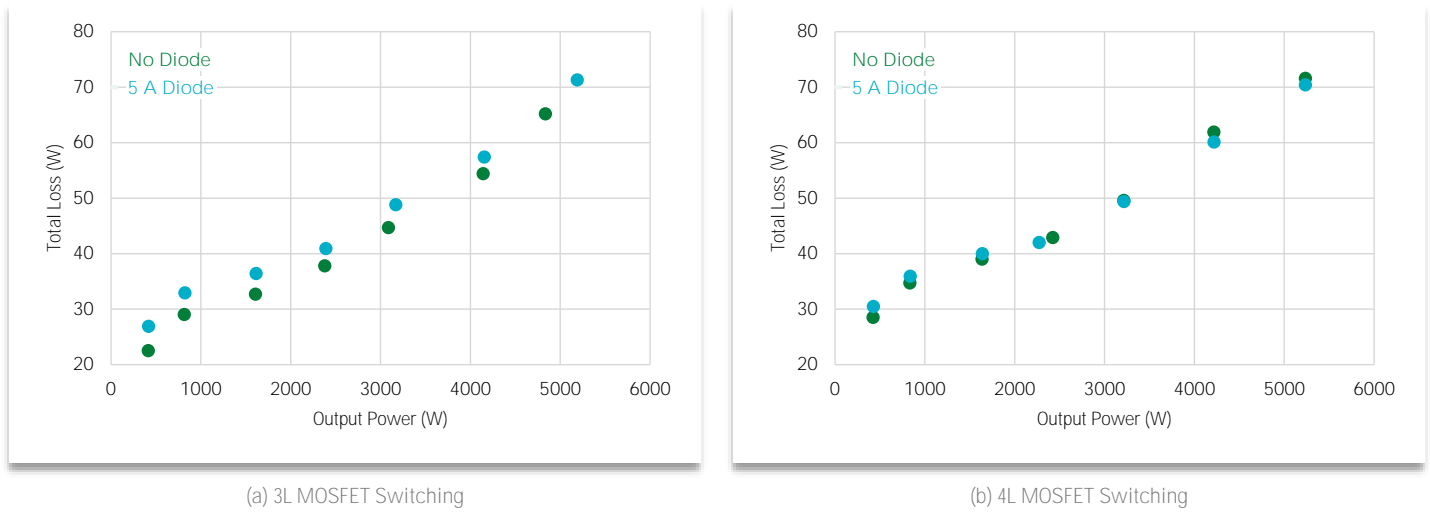


Figure 8. Converter Loss Comparison of 3L and 4L MOSFETs Switching with and without SBD as Antiparallel Diode

6. Freewheeling Device Selection

Previous test results indicate that using a higher current rating diode will increase the current overshoot during switching. A lower current rating anti-parallel diode is preferred. However, the antiparallel diode must be large enough to ensure the majority of the current conducts through anti-parallel SBD instead of the body diode of SiC MOSFET. The recommended current rating can be derived by comparing forward characteristics between SiC SBD and the SiC MOSFET body diode.

Figure 9 shows the comparison of the forward characteristics of a 1200 V 5 A SBD, the forward characteristics of a 1200 V 10 A SiC SBD, and the body diode reverse characteristics of a 1200 V 80 mOhm SiC MOSFET. Since a body diode has a P-N junction structure, the initial voltage drop is higher than SBD, but its resistance is lower due to the larger die area than SiC SBD. As the body diode and the SiC SBD are in parallel, the total current is shared to ensure that voltage across the two devices is the same. Using a 5 A rating diode as the anti-parallel diode and a 12 A total freewheeling current, the current sharing between the freewheeling diode and the MOSFET body diode will be 7 A to 5 A and the forward voltage drop will be 2.5 V. For the same 12 A total freewheeling current, if a 10 A rated SBD diode is used as the anti-parallel diode, the current share will be 10 A to 2 A and the forward voltage drop will be 2 V. Therefore, adding a 10 A diode can reduce the reverse recovery charge more effectively. But a 10 A diode will have higher output capacitance added to the body diode of the SiC MOSFET, which will increase the switching loss at light load.

Note that the current flows only through the antiparallel diode during the switching transient and dead-time period. After dead time, the SiC MOSFET channel is turned on to conduct the reverse current; therefore, the loss on antiparallel diode should be minimum and thermal management for the antiparallel diode is usually not critical. During the transition period, the current sharing also depends on the parasitic inductance in the packaging of the SiC MOSFET and antiparallel diode and power loop layout design. The static forward characteristic comparison only provides a guideline for the current rating selection.

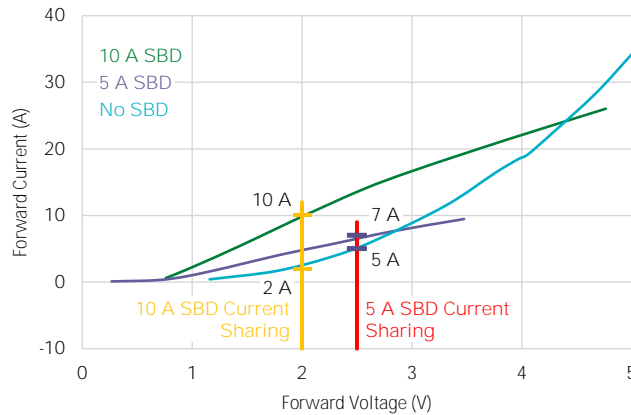


Figure 9. I-V Characteristics Comparison of SiC MOSFET Body Diode and SiC SBD

7. Conclusion

This paper discusses the optimization of freewheeling device implementation for SiC MOSFETs with Kelvin source connections. Two characterization platforms were developed to test and measure double pulse switching and continuous switching performance of a phase leg with 3L and 4L MOSFETs. Different freewheeling device implementations including SiC MOSFET body diode with and without anti-parallel SBD are presented. The switching losses and freewheeling diode results quantify the reverse recovery behavior of a 4L MOSFET’s body diode compared with that of a 3L MOSFET. Adding an antiparallel SBD to 3L packages provides limited benefits – the reduction of switching loss is only observed at heavy load and high junction temperature. At light load and low junction temperature, adding an SBD to 3L MOSFETs may even increase switching loss. Therefore, it is not recommended to add an antiparallel SBD to SiC MOSFETs without Kelvin source connection for normal applications. However, the benefit of adding SBD is more significant for SiC MOSFETs with Kelvin source connections. These benefits include turn-on loss reduction, freewheeling device voltage stress reduction, and system level EMI noise mitigation over varying working conditions. Continuous operation results also quantify the benefit of loss reduction and efficiency improvements by adding SBD. The proper selection of an SBD to optimize turn-on loss reduction is also discussed by comparing the I-V characteristics of SBD and MOSFET body diode. These results are valid for all SiC MOSFETs with Kelvin source connections including other discrete packages and power modules.

8. References

- [1] Abhijit D. Pathak, “MOSFET/IGBT Drivers Theory and Applications”, IXYS Corporation Application Notes IXAN0010, 2004
- [2] Littelfuse Corporation, “LSIC1MO120E0080 1200 V N-channel, Enhancement-mode SiC MOSFET”, Datasheet, 2017
- [3] Laszlo Balogh, “Fundamentals of MOSFET and IGBT Gate Driver Circuits,” TI. Application Report SLUA618, March 2017.
- [4] X. Zhang, “Dynamic Characterization Platform (DCP)”, Littelfuse, Application Note, Dec. 2018
- [5] X. Zhang, “Gate Driver Evaluation Platform (GDEV)”. Littelfuse, Application Note, Dec. 2019

For additional information please visit www.Littelfuse.com/powersemi

Disclaimer Notice - This document is provided by Littelfuse, Inc. ("Littelfuse") for informational and guideline purposes only. Littelfuse assumes no liability for errors or omissions in this document or for any of the information contained herein. Information is provided on an "as is" and "with all faults" basis for evaluation purposes only. Applications described are for illustrative purposes only and Littelfuse makes no representation that such applications will be suitable for the customer's specific use without further testing or modification. Littelfuse expressly disclaims all warranties, whether express, implied or statutory, including but not limited to the implied warranties of merchantability and fitness for a particular purpose, and non-infringement. It is the customer's sole responsibility to determine suitability for a particular system or use based on their own performance criteria, conditions, specific application, compatibility with other components, and environmental conditions. Customers must independently provide appropriate design and operating safeguards to minimize any risks associated with their applications and products.

Littelfuse products are not designed for, and shall not be used for, any purpose (including, without limitation, automotive, military, aerospace, medical, life-saving, life-sustaining or nuclear facility applications, devices intended for surgical implant into the body, or any other application in which the failure or lack of desired operation of the product may result in personal injury, death, or property damage) other than those expressly forth in applicable Littelfuse product documentation. Littelfuse shall not be liable for any claims or damages arising out of products used in applications not expressly intended by Littelfuse as set forth in applicable Littelfuse documentation.

Read complete Disclaimer Notice at www.littelfuse.com/disclaimer-electronics